ELSEVIER

Chemical Engineering Journal 140 (2008) 157–164

Chemical Engineering Journal

www.elsevier.com/locate/cej

Optimization of caustic current efficiency in a zero-gap advanced chlor-alkali cell with application of genetic algorithm assisted by artificial neural networks

T. Mirzazadeh [a], F. Mohammadi [b,*], M. Soltanieh [a], E. Joudaki [b]

[a] *Department of Chemical and Petroleum Engineering, Sharif University of Technology, Tehran, Iran*
[b] *Iran Polymer and Petrochemical Institute, P.O. Box 14965/115, Tehran, Iran*

Received 30 June 2007; received in revised form 5 September 2007; accepted 18 September 2007

Abstract

The effects of various process parameters on caustic current efficiency (CCE) in a zero-gap oxygen-depolarized chlor-alkali cell employing a state-of-the-art silver plated nickel screen electrode (ESNS®) were studied. For doing a thorough research, we selected the process parameters from both cathodic and anodic compartments. Seven process parameters were studied including anolyte pH, temperature, flow rate and brine concentration from the anode side, oxygen temperature and flow rate from the cathode side and the applied current density. The effect of these parameters on CCE was determined quantitatively. A feed forward neural network model with the Levenberg–Marquardt (LM) back propagation training method was developed to predict CCE. Then genetic algorithm (GA) was implemented to neural network model. The highest CCE (98.53%) was found after 20 times running GA at the following conditions: brine concentration (287 g/L), anolyte temperature (80 °C), anolyte pH (2.7), anolyte flow rate (408 cm^3/min), oxygen flow rate (841 cm^3/min), oxygen temperature (79 °C), and current density (0.33 A/cm^2).

Keywords: Advanced chlor-alkali (ACA); CCE; Process parameters; GA; Neural networks; ESNS®

1. Introduction

The progress of the membrane chlor-alkali technology and its additional optimization resulted in a meaningful reduction of energy consumption in chlor-alkali process. The state-of-the-art membrane reactors operate at voltages as low as 3.2 V at a typical current density of 0.4 A/cm^2 [1]. Brine electrolysis is still one of the most energy-intensive industrial operations, despite the tremendous efforts of the chlor-alkali industry to reduce the energy consumption. It is accepted that the developed membrane technology has reached the theoretical end-point on energy consumption. Therefore, more optimization of this process is not expected to result in a significant cut of the energy consumption. Nevertheless, by replacing the hydrogen-evolving cathode in a membrane cell with an oxygen-depolarized cathode, the cell voltage and energy consumption can be reduced by as much as 30% at 0.4 A/cm^2 [2,3]. The electrochemical reduction of oxygen in an alkaline environment has been the topic of many researches and the successful employment of silver [4–6] and platinum [5,6] catalysts in oxygen-depolarized chlor-alkali cathodes has already been reported. While an oxygen-depolarized chlor-alkali cell significantly lowers energy consumption per unit weight of chlorine and caustic, optimization of process parameters to achieve maximum current efficiency is remained almost untouched. The only published work that is somewhat related to this issue was carried out by researchers at Los Alamos National Laboratory to minimize peroxide formation in an ACA cell using ELAT® cathodes [2,3]. As far as we know, there has been no published literature on a thorough investigation of the effects of operating parameters on the CCE of ACA membrane cells. Besides, no open literature was found to explore thoroughly the performance of the newly developed ESNS®

Abbreviations: ACA, advanced chlor alkali; CCE, caustic current efficiency (%); DSA, dimensionally stable anode; ESNS, silver-plated nickel screen electrode; HF, humidifier; LM, Levenberg–Marquardt; MLP, multilayer perceptron; TK, tank.

* Corresponding author. Tel.: +98 21 44580000 19x2313; fax: +98 21 44580032.
E-mail addresses: mirzazadeh@che.sharif.edu (T. Mirzazadeh), f.mohammadi@ippi.ac.ir (F. Mohammadi), msoltanieh@sharif.edu (M. Soltanieh), e.joudaki@ippi.ac.ir (E. Joudaki).

1385-8947/$ – see front matter © 2007 Elsevier B.V. All rights reserved.
doi:10.1016/j.cej.2007.09.028

cathode by E-Tek Inc. This issue was thus chosen for further investigation.

Nevertheless, the ACA system shows a complex behavior and there is a great energy expense associated with the process parameters variations in the ACA process. A common approach to design optimization is to perform experiment with the design variables, by trial and error or one at a time, until the first feasible design is found. However, to complete the design process such an approach may be prolong and expensive when multiple factors are involved. An important issue in experimentation is how to design the experiments in order to explore and optimize the multidimensional parameter space, minimizing the number of trials required to achieve a unique solution. Approach for experimental design include techniques such as factorial designs [7], deterministic optimization algorithms like holographic search [8] and split & pool methods [9,10], or stochastic procedures like simulated annealing and genetic algorithms (GAs). Another efficient technique comprises the combination of an artificial neural network (ANN) and a GA. Thus whereas the ANN finds the internal relationship between variables in the experimental data, the optimization algorithm (GA) optimizes variables, taking into account the knowledge extracted by the ANN. The combination of the two artificial intelligence techniques is now being widely applied [11–15]. It is believed that GAs could be used as powerful techniques to solve complex and real-word problems.

This paper thus presents part of our research on the implementation of oxygen-depolarized cathodes in a modified commercial membrane cell using ESNS® cathode. The study focuses on selected performance characteristic of the cell (CCE). It is the first time that GA is implemented for optimization of CCE in ACA technology. As our study to implement gas diffusion electrode in chlor-alkali cell arose from fuel cell research, the arrangement of our ACA cell and PEM type fuel cell is relatively analogous. For example, while the most of oxygen-depolarized chlor-alkali cells [4,6,16–18] can be classified as finite gap (where the cathode side is divided by the gas-diffusion cathode into disparate oxygen and caustic compartments) we implemented a fuel cell-like, zero-gap arrangement. In this configuration, there are no independent oxygen and caustic compartments and the oxygen cathode stays in intimate contact with the ion-exchange membrane. In this way, both the flooding of the cathode by the NaOH solution and the ohmic drop have been meaningfully reduced [2,3].

2. Materials and methods

2.1. Chemicals used

The brine was prepared from analytical grade NaCl (Merck Inc.) using deionized water. All other chemicals used for analysis were also Analar grade.

2.2. Experimental set-up

The electrochemical cell was a divided filter-press type (Micro-flow cell, Electrocell AB, Sweden) with 10 cm^2 (3.3 cm × 3 cm) electrode area (Fig. 1) that was modified to allocate gas diffusion electrode. The cell used in this study employed a commercially available, 10 cm^2 gas diffusion electrodes (A2STD ESNS®) with a carbon-supported platinum catalyst (E-TEK Inc.). The catalyst layer contained 10% of carbon-supported (Vulcan XC-72) platinum with a total Pt loading of 0.6 mg cm^{-2}. The nickel screen side of the cathode remained in intimate contact with the carboxylic side of the ion exchange membrane (Flemion® 892, Asahi Glass Co.). The anode was a standard coated titanium plate (DSA®-Cl_2). The cell flow fields were made from ~2 mm Teflon. The cell performance evaluation was carried out in an ACA set-up developed in our laboratory. Fig. 2 shows the process flow diagram of the set-up used in this study. The anolyte feed tank was heated by jacketed heater and its temperature was monitored by digital thermometer. Anolyte pH was measured by an on-line pH-meter inserted in anolyte feed tank. The anolyte was recirculated in separate hydraulic circuit throughout the experiment by magnetic pump according to Fig. 2. The overflow from the anolyte compartment of the electrolysis cell was sent to a gas–liquid separator. During electrolysis, Cl_2 gas produced was absorbed by 2 M NaOH solution in TK-103 and then TK-104, respectively. The cathode chamber was fed with oxygen at atmospheric pressure. The oxygen stream was heated and humidified by a jacketed bubble column humidifier (HF). The oxygen temperature and extend of humidification was adjusted before entering the cathode compartment. In order to minimize corrosion, the cathode gas feed line was equipped with two valves that would stop the oxygen flow and replace it with nitrogen upon a power loss. Constant currents were applied to the cell and the corresponding cell voltages were measured by a multimeter. After each test, the set-up was washed thoroughly with deionized water drained and dried. Pre-

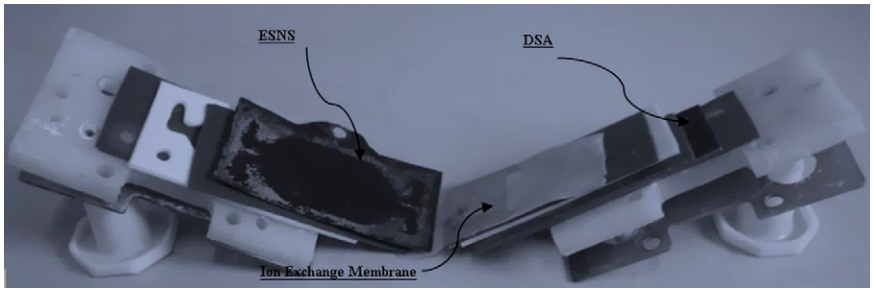

Fig. 1. Components of the membrane cell used in this study.

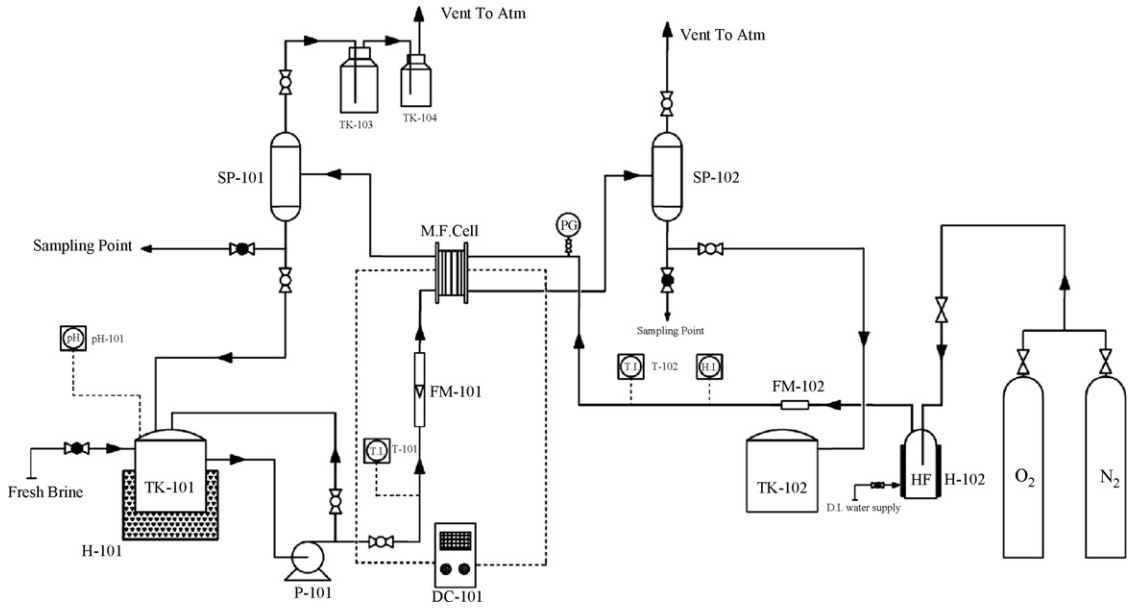

Fig. 2. Process flow diagram of the ACA set-up utilized: TK-101 (brine recirculation tank). TK-102 (NaOH product tank). TK-103, 104 (chlorine absorption tanks). SP-101, 102 (gas–liquid separator). FM-101 (liquid flow meter). FM-102 (oxygen flow meter). T-101, 102 (temperature indicator). pH-101 (on-line pH meter). DC-101 (DC power supply). H-101, 102 (jacketed electrical heater). P-101 (anolyte magnetic pump). H.I. (humidification indicator). PG (pressure gauge). HF (humidifier). M.F.Cell (membrane flow cell).

liminary tests showed in order to produce determinable chlorine and caustic, the electrolysis run time should be at least 150 min.

2.3. Analysis

CCE was determined from titration of the sodium hydroxide samples with standardized 1.0 M HCl solution (Fisher) against phenolphthalein. The peroxide content in the NaOH solution was found spectrophotometrically. Fresh samples of sodium hydroxide were mixed with a known amount of potassium ferricyanide solution in aqueous NaOH. The peroxide content was determined from a decrease of ferricyanide absorption at 418 nm [19]. Due to the very weak acidic properties of hydrogen peroxide ($pK_a = 11.75$ [20]), the volume of the acid used to neutralize the NaOH sample corresponded to the sum of the sodium hydroxide present in the sample and the NaOH produced as a result of hydro peroxide anion (HO_2^-) protonation [2]. Since the latter quantity was also equal to the amount of NaOH that would form because of HO_2^- decomposition, the CCE quoted in this study are corrected for peroxide.

2.4. Mathematical modeling and optimization

2.4.1. ANN

Artificial neural network modeling is essentially a black box operation linking input to output data using a particular set of nonlinear basis functions. ANNs consist of simple synchronous processing elements, which are inspired by biological nervous systems and the basic unit in the ANN is the neuron [21]. ANNs are trained using a large number of input data with corresponding output data (input/output pairs) obtained from actual measurement so that a particular set of inputs produces, as nearly as possible, a specific set of target outputs. Training consists of adjusting the weight associated with each connection (synapse) between neurons until the computed outputs for each set of data inputs are as close as possible to the experimental data outputs. It is well known that during the design and training of ANNs, factors such as (i) architecture of the ANN; (ii) training algorithm; and (iii) transfer function need to be considered eventually. The term "architecture of the artificial neural network" refers to the number of layers in the ANN and the number of neurons in each layer. In general, it consists of an input layer, one or more hidden layers and one output layer. The number of neurons in the input layer and the output layer are determined by the numbers of input and output parameters, respectively. In order to find the optimal architecture, number of neurons in the hidden layer has to be determined (this number will be determined based on the ANN during the training process by taking into consideration the convergence rate, mapping accuracy, etc.).

The most widely used network type is multi-layered feed-forward network trained with the back-propagation learning algorithm [22,23]. The back-propagation learning algorithm is based on the selection of a suitable error function, whose values are determined by the actual and predicted outputs of the network. The model with lowest prediction error is being used as the final and optimal model.

2.4.2. GA

These algorithms are optimization strategies developed based on the principles of natural selection. The GA begins with a population of represented random solutions in some series of structures. After this first step, a series of operators, are applied repeatedly, up to convergence is gained. In fact, the optimization strategy based in this approach can be described as a global optimization method with the benefit not to be dependent upon the initial value to achieve the convergence. Probably the most sig-

nificant drawbacks are the computer time and burden required. The GA operators are coding, reproduction, crossover and mutation. These two last operators are implemented to create new and better populations. This algorithm carries on until a termination criterion specified according to the need to achieve the goal in the optimization problem is achieved (see Fig. 3). The determination of the parameters is made through the implementation of an objective function that represents the problem in an appropriate way. The development of the GA follows some steps as coding, determination of the population size, selection (reproduction), crossover and mutation. In the binary codification, the following parameters have to be analyzed in order to achieve a good optimization algorithm performance: population sizes, chosen to be analyzed between 10 and 40; crossover operator, in two forms to know, uniform and of single-point; the selection form adopted is the tournament one [24]. The elitism and the mutation (Jump and Creep mutation) are fixed values.

3. Results and discussion

A great number of experiments were carried out in this study to examine the effect of each process parameter separately. In each series of experiments, only one process parameter was changed and the others were fixed. After that, a multilayer perceptron neural network, with seven input nodes, ten nodes in the hidden layer, and one output node, was developed to relate experimental data (Fig. 4). In the training step, a larger part of the data (80%) was used to train the model with the LM back propagation training method and the remaining data (20%) were used for validation. Indeed, 60 experiments were done and 42 data were chosen for training and validation of the neural network. The nodes in hidden layers did the mapping function of MLP. Their number was chosen to avoid under or over fitting. The initial weights of the neural network were chosen randomly between [−1, 1]. The parameters modified iteratively until convergence was reached.

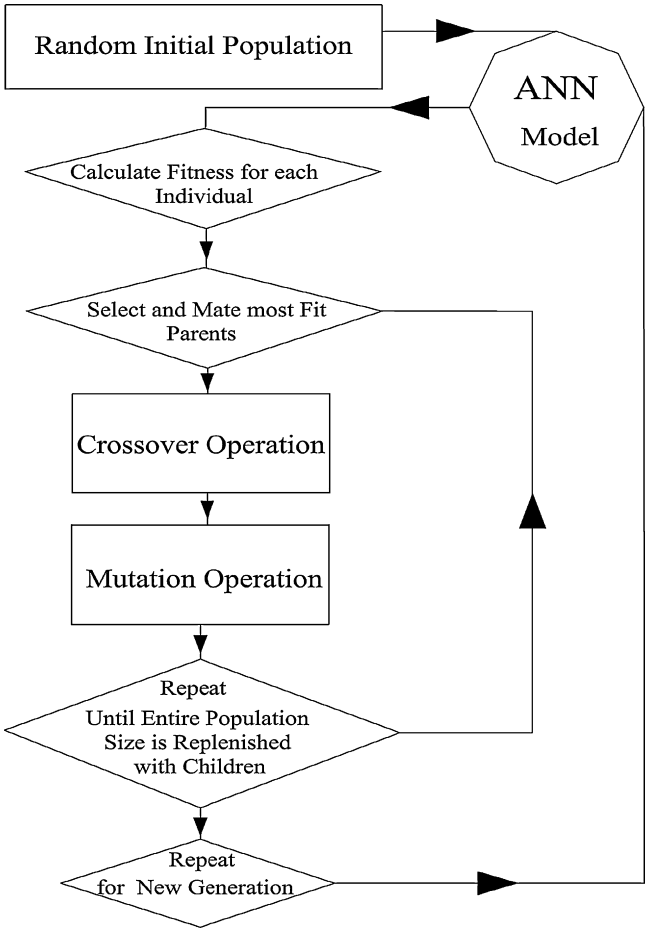

Fig. 3. GA developed in this study.

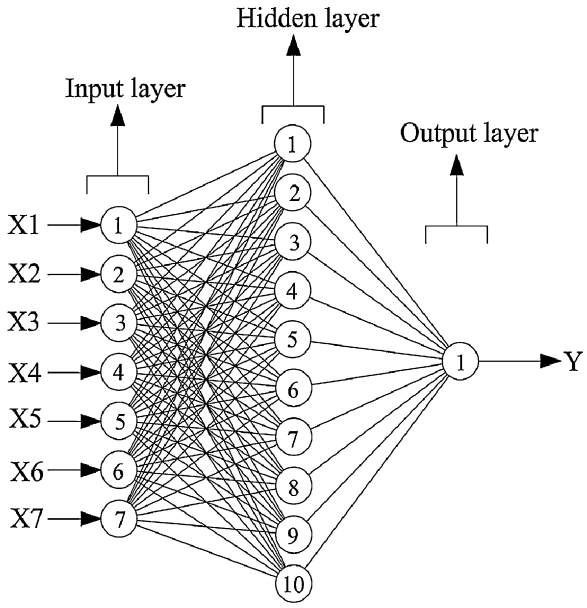

Fig. 4. ANN model utilized in this study.

3.1. Effect of brine concentration

The effect of brine concentration on CCE was studied and the results are shown in Fig. 5. As seen, like conventional membrane cells [25] and like ACA zero-gap cells with ELAT® [2,3], the CCE increases linearly with brine concentration within the experimental range studied. A good agreement between exper-

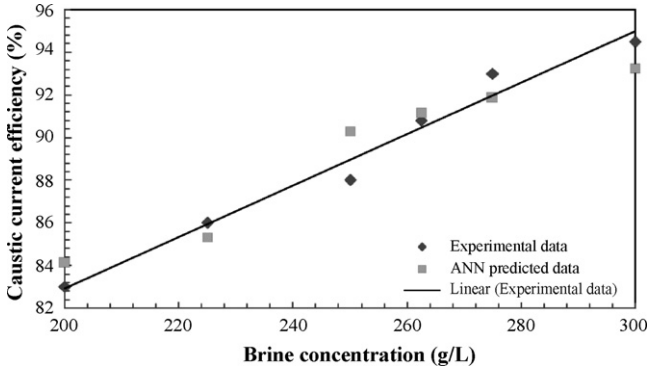

Fig. 5. The effect of brine concentration on CCE at anolyte: temperature (80 °C), pH (2.5), flow rate (350 cm^3/min), oxygen: flow rate (700 cm^3/min), temperature (80 °C), and current density (0.2 A/cm^2).

imental data and the predicted ANN results can be seen. At low brine concentrations, the low CCE is due to the membrane swelling and permeability. Consequently, more water is transported through the membrane yielding lower caustic concentration [26]. As could be expected, the CCE also increases with brine concentration because of decreased caustic crossover through the membrane. One may suspect the partial oxygen evolution [27,28] on the DSA® anode to contribute to the above phenomena. This reaction produces hydronium cations and its relative contribution to the measured current increases with the decrease in brine concentration [27,28].

3.2. Effect of anolyte pH

This is the first time that the effect of anolyte pH on CCE of an ACA cell is being studied. The corresponding results are represented in Fig. 6. The similarity between experimental data and ANN predicted data is obvious. The results show that CCE increases with increasing anolyte pH within the experimental range studied. It is believed that an increase in brine acidity (decease in pH) may produce an increased H_3O^+ flux across the membrane, which may result in a low membrane resistance, low CCE and low NaOH concentration. However, like conventional membrane cells reported earlier [25] the chlorine current efficiency decreases with increasing brine pH due to the production of by products such as hypochlorite and chlorate in anolyte at higher pH's [29].

3.3. Effects of anolyte and oxygen temperature

The non-isothermal effect of an ACA cell was studied for the first time and the results are shown in Figs. 7 and 8. We did not see a very good agreement between experimental data and ANN predicted data in both cases especially for oxygen temperature. This may be due to the low precision of some experimental data because of hard experimental conditions. The result shows that CCE increases with temperature in both cases. At low temperatures, the rate of oxygen reduction is low and this lowers CCE profoundly [25]. Another point that should mention is that the electrical conductivity of the electrolyte is a function of concentration and temperature. At high temperatures, the high conductivity of anolyte solution lowers the cell voltage and therefore energy consumption of the chlor-alkali set-up will be low as conventional membrane cells [25]. Consequently the economic and energy factors are in favor of the technology that utilizes higher temperatures.

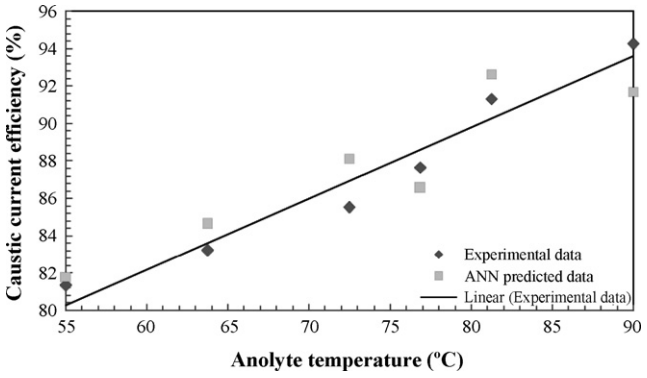

Fig. 7. The effect of anolyte temperature on CCE at anolyte: concentration (230 g/L), pH (2.5), flow rate (350 cm^3/min), oxygen: flow rate (900 cm^3/min), temperature (75 °C), and current density (0.2 A/cm^2).

3.4. Effects of anolyte and oxygen flow rates

To see the effects of anolyte and oxygen flow rates on performance of ACA cells, we studied each parameter individually. As seen (Figs. 9 and 10), the agreement between experimental data and ANN predicted data is good. By increasing anolyte flow rate (velocity), CCE increases. This result is in complete agreement with the conventional membrane cells [25]. This may be because the amount of attached Cl_2 bubbles on anodic side of the membrane and those remained within anolyte are reduced [30,31]. In fact, the bubbles decrease the effective area of the membrane by blinding effects especially at low anolyte flow rates. The effect of oxygen flow rate on CCE was not linear also. The results shows that CCE increases with increasing oxygen flow rate as what observed with ELAT® [2,3]. The increase of CCE at higher rates of oxygen flow rate most likely results from the effect of gas flow on the effectiveness of caustic removal from the electrode. High gas velocity in the cathode chamber makes the removal of

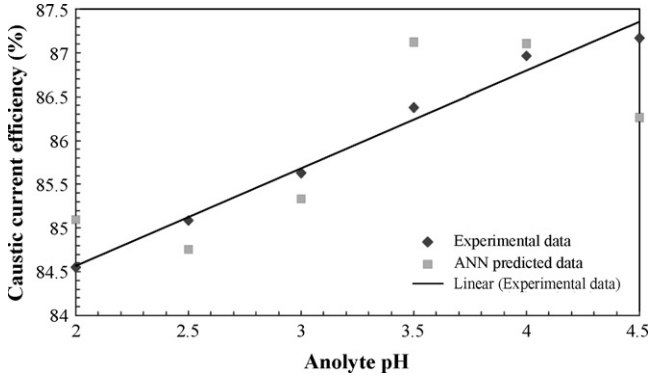

Fig. 6. The effect of anolyte pH on CCE at anolyte: concentration (210 g/L) temperature (75 °C), flow rate (350 cm^3/min), oxygen: flow rate (500 cm^3/min), temperature (75 °C), and current density (0.2 A/cm^2).

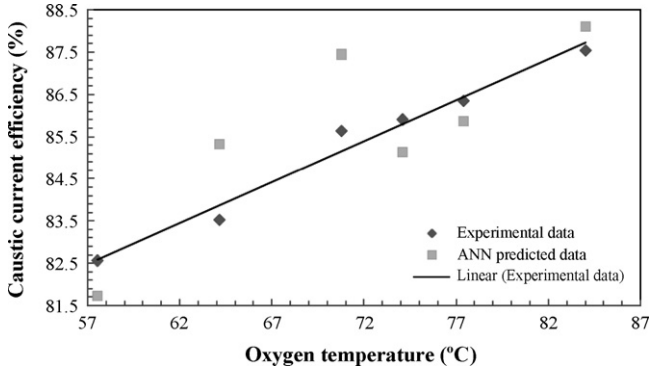

Fig. 8. The effect of oxygen temperature on CCE at anolyte: concentration (230 g/L), pH (2.5), flow rate (250 cm^3/min), temperature (70 °C), oxygen: flow rate (500 cm^3/min), and current density (0.2 A/cm^2).

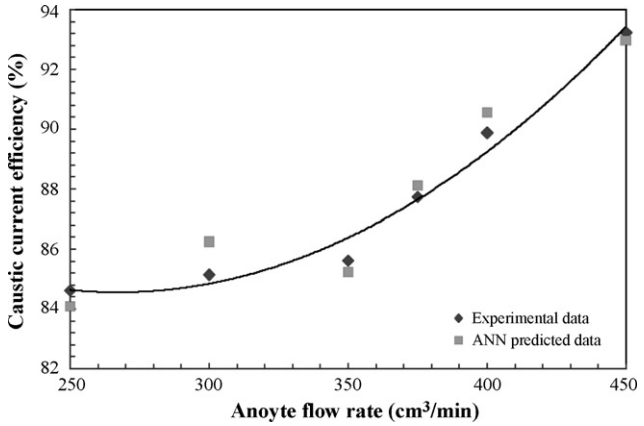

Fig. 9. The effect of anolyte flow rate on CCE at anolyte: concentration (280 g/L), pH (2.5), temperature (75 °C), oxygen: flow rate (700 cm^3/min), temperature (75 °C), and current density (0.3 A/cm^2).

caustic from the electrode pores easier than low velocities. In very low gas velocities, we had accumulation of viscous caustic in the cathode chamber.

3.5. Effect of current density

The cell was operated at six current densities between 0.1 and 0.4 A/cm^2 as industrial membrane cells. The results (Fig. 11) show that the agreement between experimental data and ANN predicted data is good. The decrease in CCE with increasing current density is similar to ELAT® results especially at low current density [2,3]. Effect of current density on CCE is believed to originate from the different kinetics of desirable complete 4-electron reduction and unwanted partial 2-electron reduction of oxygen:

$$O_2 + 2H_2O + 4e \rightarrow 4OH^- \quad (1)$$

$$O_2 + H_2O + 2e \rightarrow OOH^- + OH^- \quad (2)$$

In fact, the increase of current density shifts the cathode potential towards the more negative values and this phenomenon affects the relative rates of the two reactions. Higher current densities are likely to decrease CCE by increasing membrane swelling

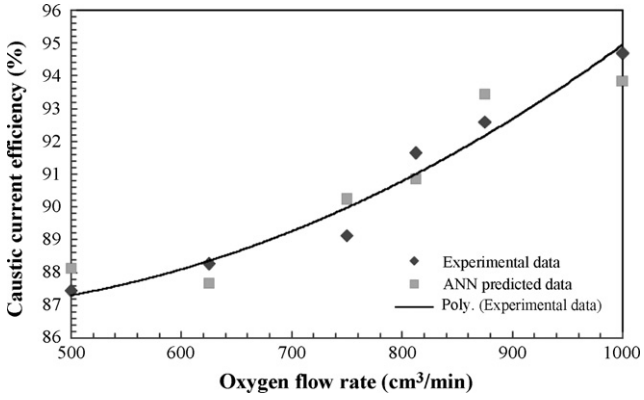

Fig. 10. The effect of oxygen flow rate on CCE at anolyte: concentration (250 g/L), pH (2.5), flow rate (400 cm^3/min), temperature (70 °C), oxygen: temperature (70 °C), and current density (0.15 A/cm^2).

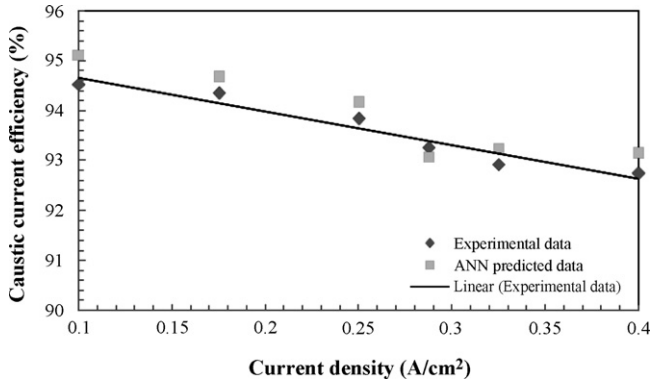

Fig. 11. The effect of current density on CCE at anolyte: concentration (270 g/L), pH (3), flow rate (450 cm^3/min), temperature (80 °C), oxygen: temperature (80 °C), flow rate (800 cm^3/min).

and permeability [26], by more significant contribution of the oxygen evolution reaction as well as by membrane blinding by chlorine gas in anode side.

3.6. Optimization of CCE

The optimization using the ANN model instead of mathematical modeling took into account operational conditions of the ACA cell. The chosen parameters to implement the optimization were those with more sensitivity in the chlor-alkali process. The objective is to maximize CCE, using as main variables the brine concentration, the anolyte temperature, the anolyte pH, the anolyte flow rate, the oxygen flow rate, the oxygen temperature and the current density, in seven variables. All other variables such as the extent of humidification and time were fixed (saturated oxygen and 150 min). In this way, the objective function applied to the optimization is the CCE. Table 1 shows the valid parameters limits to be optimized according to the experimental data. The parameters to be optimized were codified with the binary form, based and adapted of many published literature works [32–34]. In genetic algorithm, the continuous form was used with Gradient Descent method. Table 2 shows the selected genetic algorithm control parameters for the ACA process.

ANN and GA were implemented using M-file script programming in MATLAB platform. After 20 times running the genetic algorithm and using the average of the results, CCE reached 98.53%. Table 3 shows the optimization results. To examine the results we ran the ACA set-up near the optimum point and the corresponding CCE was 97.67%.

Table 1
Limits of validity of the operational parameters to be optimized

Process parameters	Lower limits	Upper limits
Brine concentration (g/L)	200	300
Anolyte temperature (°C)	55	90
Anolyte pH	2	4.5
Anolyte flow rate (cm^3/min)	250	450
Oxygen flow rate (cm^3/min)	500	1000
Oxygen temperature (°C)	57.5	84
Current density (A/cm^2)	0.1	0.4

Table 2
Parameters of genetic algorithm utilized in the optimization

Genetic parameters	Values
Population size	20
Uniform crossover and single-point (%)	80
Jump mutation rate (%)	1
Creep mutation (%)	2
Generations	250

Table 3
The results of optimization by GA

Process parameters	Value
Brine concentration (g/L)	287
Anolyte temperature (°C)	80
Anolyte pH	2.7
Anolyte flow rate (cm^3/min)	408
Oxygen flow rate (cm^3/min)	841.4
Oxygen temperature (°C)	79
Current density (A/cm^2)	0.33
Caustic current efficiency (%)	98.53

4. Conclusion

In this study, a modified commercial electrochemical cell with the state-of-the-art ESNS® cathode has been optimized to maximize CCE. Optimization problem was included two steps. In step, one, instead of using the mathematical modeling, a multilayer perceptron neural network with the LM back propagation training algorithm was implemented to relate experimental data. In this step we studied the effects of seven process parameters individually also. The experimental results revealed that CCE increases by increasing in brine concentration and anolyte and oxygen temperatures and flow rates and decreases by increasing in current density within the experimental range studied. The results showed that it is not necessary to pressurize ESNS® contrary to ELAT® [2,3] in ACA zero-gap cells. A good agreement between experimental data and the predicted ANN results was seen except for oxygen temperature data. In step two, the genetic algorithm was used as powerful optimization technique, which gave good solutions for this problem. A simple GA was used in this study to search the seven-dimensional spaces. The population size used was 20 as recommended [32]. The crossover rate of 80% was satisfactory to supply good results. The program of optimization was run for 20 times. The average obtained CCE was generally comparable with the current industrial standard for membrane cells, i.e. 93–95%. The closeness of corresponding anolyte and oxygen temperatures shows that non-isothermal operation of ACA cell would not maximize CCE.

Acknowledgements

The optimization of advanced chlor-alkali technology with using state-of-the-art ESNS® would not have been possible without the financial support of the Iran Polymer and Petrochemical Institute. The authors are grateful to Dr. Jerzy Chlistunoff from Los Alamos National Laboratory for frequent discussion and patient helps during this project and to Amin Fakhrazari form Department of Mechanical Engineering of Sharif University of Technology.

References

[1] K. Yamaguchi, Chlor-alkali technologies applied in Japan, in: H.S. Burney, N. Furuya, F. Hine, K.-I. Ota (Eds.), Chlor-Alkali and Chlorate Technology: R.B. MacMullin Memorial Symposium, 196th Meeting of the Electrochemical Society, vol. 99-21, Hawaii, October, Electrochemical Society Proceedings, 1999, pp. 127–144.
[2] L. Lipp, S. Gottesfield, J. Chlistunoff, J. Appl. Electrochem. 35 (10) (2005) 1015–1021.
[3] J. Chlistunoff, Advanced Chlor-Alkali Technology, Final technical report, Los Alamos National Laboratory, New Mexico, United States, 2004.
[4] R. Beckmann, B. Lüke, Know-how and technology—improving the return on investment for conversions, expansions and new chlorine plants, in: J. Moor House (Ed.), Modern Chlor-Alkali Technology, Proceedings of the 2000 London International Chlorine Symposium Organized by SCI's Electrochemical Technology Group, vol. 8, London, UK, 31st May–2nd June, Blackwell Science, 2001, 2000, pp. 196–212.
[5] N. Furuya, H. Aikawa, Electrochim. Acta 45 (25/26) (2000) 4251.
[6] F. Federico, G.N. Martelli, D. Pinter, Gas-diffusion electrodes for chlorine-related (production) technologies, in: J. Moor House (Ed.), Modern Chlor-Alkali Technology, Proceedings of the 2000 London International Chlorine Symposium Organized by SCI's Electrochemical Technology Group, London, UK, 31st May–2nd June, Blackwell Science, 2001, 2000, pp. 114–127.
[7] D.C. Montgomery, Design and Analysis of Experiments, Wiley, New York, 2001.
[8] L. Végvári, A. Tomposb, S. Gobölösb, J. Margitfalvi, Catal. Today 81 (3) (2003) 517–527.
[9] J. Klein, T.Z. Ech, J.M. Newsam, S.A. Schunk, Appl. Catal. 254 (1) (2003) 121–131.
[10] M.A. Aramendía, V. Borau, C. Jiménez, J.M. Marinas, F.J. Romero, F.J. Urbano, J. Catal. 209 (2) (2002) 413–416.
[11] C. Klanner, D. Farrusseng, L. Baumes, C. Mirodatos, F. Schueth, Qsadr. Comb. Sci. 22 (7) (2003) 729–736.
[12] F. Gilardoni, A. Graham, B. McKay, B. Brown, Proceedings of the 225th ACS National Meeting, New Orleans, USA, March 23–27, 2003.
[13] L. Baumes, D. Farrusseng, M. Lengliz, C. Mirodatos, Using artificial neural networks to boost high-throughput discovery in heterogeneous catalysis, Qsadr. Comb. Sci., in press.
[14] D. Farrusseng, L. Baumes, C. Mirodatos, in: R.A. Potyrailo, E.J. Amis (Eds.), High-Throughput Analysis: A Tool for Combinatorial Materials Science, Kluwer-Academic/Plenum, 2003, pp. 551–579.
[15] C. Klanner, D. Farrusseng, L. Baumes, C. Mirodatos, F. Schueth, Angew. Chem. Int. Ed. 43 (40) (2004) 5347–5349.
[16] A. Sakata, M. Kato, K. Hayashi, H. Aikawa, K. Saiki, Long term performances of gas diffusion electrode in laboratory cells, in: H.S. Burney, N. Furuya, F. Hine, K.-I. Ota (Eds.), Proceedings of the Chlor-Alkali and Chlorate Technology: R.B. MacMullin Memorial Symposium, 196th Meeting of the Electrochemical Society, vol. 99-21, Hawaii, October, Electrochemical Society Proceedings, 1999, pp. 223–233.
[17] O. Ichinose, H. Aikawa, T. Watanabe, A. Uchimura, Pilot cell scale manufacture of the gas diffusion electrode, in: H.S. Burney, N. Furuya, F. Hine, K.-I. Ota (Eds.), Proceedings of the Chlor-Alkali and Chlorate Technology: R.B. MacMullin Memorial Symposium, 196th Meeting of the Electrochemical Society, vol. 99-21, Hawaii, October, Electrochemical Society Proceedings, 1999, pp. 216–222.
[18] K. Saiki, A. Sakata, H. Aikawa, N. Furuya, Reduction in power consumption of chlor-alkali membrane cell using oxygen depolarized cathode, in: H.S. Burney, N. Furuya, F. Hine, K.-I. Ota (Eds.), Proceedings of the Chlor-Alkali and Chlorate Technology: R.B. MacMullin Memorial Symposium, 196th Meeting of the Electrochemical Society, vol. 99-21, Hawaii, October, Electrochemical Society Proceedings, 1999, pp. 188–195.
[19] F. Aziz, G.A. Mirza, Talanta 11 (1964) 889.

[20] M. Ardon, in: R.A. Plane, M.J. Sienko (Eds.), Oxygen Elementary Forms and Hydrogen Peroxide, the Physical Inorganic Chemistry Series, W.A. Benjamin, New York, 1965.
[21] R. Beale, T. Jackson, Neural Computing: An Introduction, Adam Hilger, Bristol, 1990.
[22] J.A. Freeman, D.M. Skapura, Neural Networks, Algorithms, Applications, and Programming Techniques, Addison-Wesley, Massachusetts, 1992.
[23] S. Haykin, Neural Networks, A Comprehensive Foundation, Prentice Hall, Upper Saddle River, New Jersey, 1994.
[24] I.R.S. Victorino, J.P. Maia, E.R. Morais, M.R. Wolf Maciel, R. Maciel Filho, Chem. Eng. J. 132 (1–3) (2007) 2–3.
[25] A.A. Jalali, M.Sc. Thesis, Iran University of Science and Technology, Department of Chemical Engineering, 2005.
[26] J.T. Keating, H.M.B. Gerner, High current density operation—the behavior of ion exchange membranes in chloralkali electrolyzers, in: S. Sealey (Ed.), Modern Chlor-Alkali Technology, Proceedings of the 1997 London International Chlorine Symposium Organized by SCI Electrochemical Technology Group, vol. 7, London, UK, 4th–6th June, SCI 1998, 1997, pp. 135–144.
[27] L.R. Czarnetzki, L.J.J. Janssen, J. Appl. Electrochem. 22 (4) (1992) 315.
[28] J.L. Fernández, M.R. Gennero de Chialvo, A.C. Chialvo, J. Appl. Electrochem. 32 (5) (2002) 513.
[29] D. Bergner, J. Appl. Electrochem. 20 (3) (1990) 716–722.
[30] J. St. Pierre, A. Wragg, Electrochim. Acta 38 (13) (1993) 1705–1710.
[31] Y. Xiong, L. Jialing, S. Hong, J. Appl. Electrochem. 22 (12) (1992) 486–490.
[32] D.L. Carroli, AIAA J. 34 (2) (1996) 338–346.
[33] K. Deb, Genetic algorithms in search and optimization: the technique and applications, in: Proceedings of the International Workshop on Soft Computing and Intelligent Systems, Calcutta, India, Machine Intelligence Unit, Indian Statistical Institute, 1998, pp. 58–87.
[34] D.E. Goldberg, Genetic Algorithms in Search, Optimization and Machine Learning, Addison-Wesley, MA, 1989.